

Mode-dependent Loss and Gain Estimation in SDM Transmission Based on MMSE Equalizers

Ruby S. B. Ospina, *Student Member, OSA*, Menno van den Hout, *Student Member, IEEE*,

Juan Carlos Alvarado-Zacarias, *Student Member, IEEE*, Jose Enrique Antonio-López, Marianne Bigot-Astruc,

Adrian Amezcua Correa, Pierre Sillard, *Member, IEEE*, Rodrigo Amezcua-Correa, *Member, IEEE*,

Chigo Okonkwo, *Senior Member, IEEE*, and Darli A. A. Mello, *Member, IEEE*

Abstract—The capacity in space division multiplexing (SDM) systems with coupled channels is fundamentally limited by mode-dependent loss (MDL) and mode-dependent gain (MDG) generated in components and amplifiers. In these systems, MDL/MDG must be accurately estimated for performance analysis and troubleshooting. Most recent demonstrations of SDM with coupled channels perform MDL/MDG estimation by digital signal processing (DSP) techniques based on the coefficients of multiple-input multiple-output (MIMO) adaptive equalizers. Although these methods provide a valid indication of the order of magnitude of the accumulated MDL/MDG over the link, MIMO equalizers are usually updated according to the minimum mean square error (MMSE) criterion, which is known to depend on the channel signal-to-noise ratio (SNR). Therefore, MDL/MDG estimation techniques based on the adaptive filter coefficients are also impaired by noise. In this paper, we model analytically the influence of the SNR on DSP-based MDL/MDG estimation, and show that the technique is prone to errors. Based on the transfer function of MIMO MMSE equalizers, and assuming a known SNR, we calculate a correction factor that improves the estimation process in moderate levels of MDL/MDG and SNR. The correction factor is validated by simulation of a 6-mode long-haul transmission link, and experimentally using a 3-mode transmission link. The results confirm the limitations of the standard estimation method in scenarios of high additive noise and MDL/MDG, and indicate the correction factor as a possible solution in practical SDM scenarios.

Index Terms—Mode-dependent loss, mode-dependent gain, space division multiplexing, optical fiber communications.

Manuscript received XXX xx, XXXX; revised XXXXX xx, XXXX; accepted XXXX XX, XXXX. Date of publication XXXX XX, XXXX. This work was partially supported by FAPESP under grants 2018/25414-6, 2018/14026-5, 2017/25537-8, 2015/24341-7, 2015/ 24517-8 and by the TU/e-KPN flagship Smart Two project. This article was presented in part at the Optical Fiber Communications Conference, San Diego, CA, USA, Mar. 2020.

R. S. B. Ospina and D. A. A. Mello are with the School of Electrical and Computer Engineering, State University of Campinas, Campinas 13083-970, Brazil (e-mail: r163653@dac.unicamp.br, darli@unicamp.br).

M. van den Hout and C. Okonkwo are with the High Capacity Optical Transmission Laboratory, Electro-Optical Communications Group, Eindhoven University of Technology, PO Box 513, 5600 MB, Eindhoven, The Netherlands. (e-mail: {m.v.d.hout; c.m.okonkwo}@tue.nl).

J.C. Alvarado-Zacarias, J.E. Antonio-López and R. Amezcua-Correa are with the CREOL, The College of Optics and Photonics, University of Central Florida, Orlando, 32816, USA (e-mail: jcalvarazac@knights.ucf.edu, jealopez@creol.ucf.edu, r.amezcua@creol.ucf.edu)

M. Bigot-Astruc, A. Amezcua Correa and P. Sillard are with Prysmian Group, 644 Boulevard Est, Billy Berclau, 62092 Haisnes Cedex, France. (e-mail: {Marianne.Bigot; Adrian.amezcua; Pierre.Sillard}@prysmiangroup.com)

Color versions of one or more figures in this paper are available online at <http://ieeexplore.ieee.org>.

Digital Object Identifier xxxxxxxxxxxxxxxxxxxxxxxxx

I. INTRODUCTION

SPACE division multiplexing (SDM) enables significant increase in capacity and integration at the component, fiber and system level [1]. In recent years, several SDM flavors have been proposed over single-mode fiber bundles [2], [3], uncoupled or coupled multi-core fibers (MCFs) [4], [5], multi-mode fibers (MMFs), few-mode fibers (FMFs) [6], or few-mode multi-core fibers (FM-MCFs) [7]. SDM long-haul transmission with coupled channels demands multiple-input multiple-output (MIMO) equalizers at reception to compensate for any linear mixing between modes. In addition to linear coupling and modal dispersion, the guided modes may be subject to unequal attenuation and amplification. This effect is known as mode-dependent loss (MDL) and mode-dependent gain (MDG). MDL/MDG turn the channel capacity into a random variable, reducing the average channel capacity and generating outages [8]. The combined effect of accumulated MDL/MDG and amplifier noise fundamentally limits the performance of high-capacity SDM systems to be deployed at long distances. The impact of MDL/MDG on the channel capacity of coupled SDM transmission has been widely investigated. In [8], Ho *et al.* present a statistical characterization of MDL and quantify its effect on the channel capacity in strongly coupled SDM systems. In [9], Winzer *et al.* discuss the MDL-induced capacity reduction in SDM channels and provide closed-form expressions for the system outage performance. In [10], Mello *et al.* review analytical expressions for channel capacity in MDG-impaired SDM systems. Moreover, they study the effect of frequency diversity on the MDG-induced outage probability and quantify the maximum tolerable per-amplifier MDG for a certain average capacity metric in ultra-long-haul (ULH) systems.

Digital signal processing (DSP)-based estimation of MDL/MDG by coherent receivers yields a two-fold benefit namely: assessing the link performance and estimating a lower bound on the per-amplifier MDG performance. In DSP-based MDL/MDG estimation, the channel transfer function is usually estimated by the inverse frequency response of the MIMO equalizer. In [6], Van Weerdenburg *et al.* presents the evolution with distance of the MDL estimated with a 12×12 least mean square (LMS) MIMO equalizer in a 138-Tb/s 6-mode transmission. In [11], the same authors discuss the DSP-based MDL estimation over 120 wavelength channels throughout the C-band in a 650 km 6-mode transmission. In [12], Rademacher

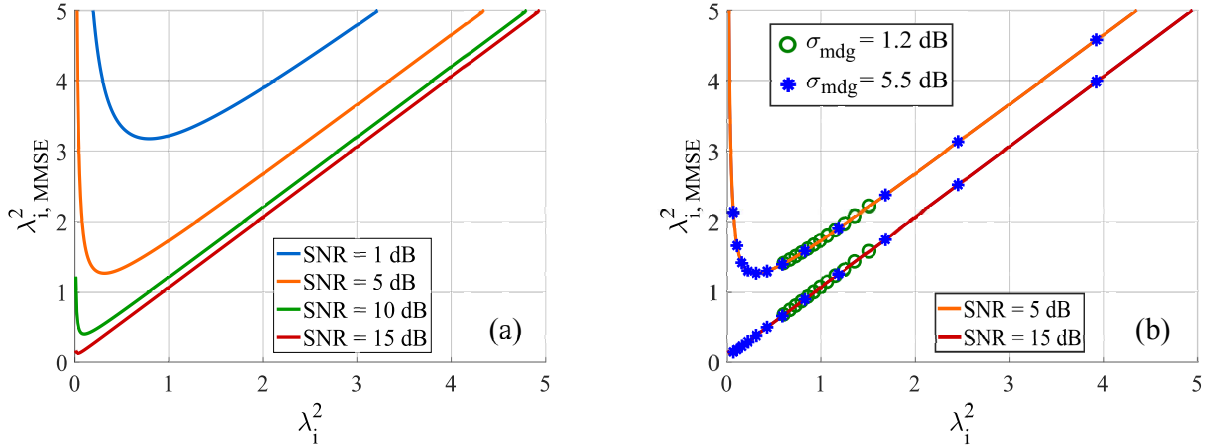


Fig. 1. (a) Eigenvalues estimated by DSP, $\lambda_{i, \text{MMSE}}^2$, as a function of the actual eigenvalues λ_i^2 for different levels of SNR. (b) Distribution of the 12 eigenvalues of a 6 spatial modes channel at two different levels of MDL/MDG and SNR.

et al. use the coefficients of a 6×6 MIMO equalizer to estimate the MDL at different modal launch powers in a 3-mode transmission. Also, recently in [13], Rademacher *et al.* estimate the MDL in a 38-core-3-mode transmission by employing a 6×6 MIMO equalizer to process each core.

We showed in [14] that, as adaptive MIMO equalizers typically use the minimum mean square error (MMSE) criterion [15], the MDL/MDG estimation accuracy is affected by the channel signal-to-noise ratio (SNR). Using the analytical transfer function of MMSE equalizers, we also show that MDL/MDG estimation errors can be partially compensated by a correction factor based on a known SNR. The results are validated by Monte-Carlo simulation. In this paper, we extend the results of [14], by addressing the problem in more detail and validating the method experimentally using a 3-mode transmission link.

The remainder of this paper is divided as follows. Section II covers the fundamentals of DSP-based MDL/MDG estimation and derives the correction factor adopted to enhance the estimation accuracy. Section III presents the validation of the correction factor by simulations of a 6-mode long-haul transmission. Section IV describes the experimental setup for a 3-mode transmission link. Section V presents the experimental results obtained with the 3-mode transmission link. Lastly, Section VI concludes the paper.

II. DSP-BASED MODE-DEPENDENT LOSS AND GAIN ESTIMATION

SDM optical systems with coupled channels deployed at long distances will require multiple inline amplifiers that may present a different gain profile for the various guided spatial modes, resulting in MDG. Moreover, fiber bends, connectors, splices, and optical devices, such as multiplexers, also introduce MDL. The MDL/MDG of a link can be computed from the eigenvalues λ_i^2 of the operator $\mathbf{H}\mathbf{H}^H$, where \mathbf{H} is the channel transfer matrix, and $(\cdot)^H$ denotes the Hermitian transpose operator [9], [8]. MDL/MDG is usually quantified by two possible metrics. In links with weak mode coupling,

the peak-to-peak value, given by the ratio between the highest and the lowest eigenvalues in dB, is a relevant metric [9], [16]. On the other hand, the standard deviation of the eigenvalues in logarithmic scale, σ_{mdg} , is usually employed to characterize the MDL/MDG in links with strong mode coupling [8], [10], [17]. In this paper, we focus on the standard deviation metric because of its direct applicability in long-distance links [17]. In DSP-based MDL/MDG estimation, the channel transfer matrix \mathbf{H} is usually estimated from the MIMO equalizer transfer function \mathbf{W} [6], [12], [13]. The MMSE equalizer transfer function can be expressed as [18], [19]

$$\mathbf{W}_{\text{MMSE}} = \left(\frac{\mathbf{I}}{\text{SNR}} + \mathbf{H}^H \mathbf{H} \right)^{-1} \mathbf{H}^H. \quad (1)$$

The SNR in (1) is the electrical SNR calculated before the MIMO equalizer, and is equivalent to the optical SNR (OSNR) calculated using the signal bandwidth as reference bandwidth. As DSP-based MDL/MDG estimation uses $\mathbf{W}_{\text{MMSE}}^{-1}$ as an estimate of \mathbf{H} , the eigenvalues λ_i^2 are estimated from the eigenvalues of $\mathbf{W}_{\text{MMSE}}^{-1} (\mathbf{W}_{\text{MMSE}}^{-1})^H$. The relationship between the actual eigenvalues λ_i^2 and the eigenvalues obtained by DSP, $\lambda_{i, \text{MMSE}}^2$, can be obtained from the eigendecomposition of $\mathbf{W}_{\text{MMSE}}^{-1} (\mathbf{W}_{\text{MMSE}}^{-1})^H$, as

$$\begin{aligned} \mathbf{W}_{\text{MMSE}}^{-1} (\mathbf{W}_{\text{MMSE}}^{-1})^H &= \frac{(\mathbf{H}\mathbf{H}^H)^{-1}}{\text{SNR}^2} + \frac{2\mathbf{I}}{\text{SNR}} + \mathbf{H}\mathbf{H}^H \\ &= \mathbf{Q} \left[\frac{\mathbf{\Lambda}_H^{-1}}{\text{SNR}^2} + \frac{2\mathbf{I}}{\text{SNR}} + \mathbf{\Lambda}_H \right] \mathbf{Q}^{-1}, \end{aligned} \quad (2)$$

where $\mathbf{\Lambda}_H$ is a diagonal matrix whose main diagonal has elements λ_i^2 , and \mathbf{Q} is a matrix whose columns are the eigenvectors of $\mathbf{H}\mathbf{H}^H$. From (2), the original eigenvalues λ_i^2 , and the eigenvalues obtained by DSP, $\lambda_{i, \text{MMSE}}^2$, are related by [14]

$$\lambda_{i, \text{MMSE}}^2 = \left[\frac{(\lambda_i^2)^{-1}}{\text{SNR}^2} + \frac{2}{\text{SNR}} + \lambda_i^2 \right], \quad (3)$$

Fig. 1a shows $\lambda_{i, \text{MMSE}}^2$ as a function of λ_i^2 for different levels of SNR. At high SNR, the first term in (3) tends

to zero, and λ_i^2 and $\lambda_{i\text{MMSE}}^2$ are linearly related with linear coefficient $2/\text{SNR}$. As the SNR decreases, lower values of λ_i^2 start to raise, breaking the linear relation, further impairing the estimation process. Fig. 1b illustrates the same effect, indicating by markers the eigenvalues obtained by different realizations of MDL/MDG and SNR in a system with 6 spatial modes (12 spatial and polarization modes). At SNR = 15 dB, the eigenvalues are positioned on the $x = y$ curve, and the conventional estimation process is successful. At SNR = 5 dB and $\sigma_{\text{mdg}} = 1.2$ dB, the estimated eigenvalues are simply displaced by $2/\text{SNR}$. If the SNR is known, this displacement can be corrected. At SNR = 5 dB and $\sigma_{\text{mdg}} = 5.5$ dB, the eigenvalues λ_i^2 in blue asterisks disperse and the lower estimated eigenvalues raise because of the nonlinear term. In this condition, the estimation accuracy of the standard DSP-based method is strongly affected.

If the SNR is known, (3) can be inverted to recover λ_i^2 from $\lambda_{i\text{MMSE}}^2$, resulting in a quadratic equation with two roots

$$\lambda_i^2 = \frac{[\text{SNR}^2 \lambda_{i\text{MMSE}}^2 - 2 \text{SNR}] \pm \sqrt{[\text{SNR}^2 \lambda_{i\text{MMSE}}^2 - 2 \text{SNR}]^2 - 4 \text{SNR}^2}}{2 \text{SNR}^2}. \quad (4)$$

The highest solution of (4) recovers λ_i^2 for high and moderate values of SNR and low and moderate values of MDL/MDG. In this paper, we adopt such positive solution as a correction factor applied over the DSP eigenvalues, $\lambda_{i\text{MMSE}}^2$, to enhance the MDL/MDG estimation process.

The expression for the MMSE equalizer in (1) and the correction of the estimated eigenvalues by (4) apply to any coupled system represented by a transfer matrix \mathbf{H} , irrespective if it operates in the regimes of weak or strong mode coupling. In this paper, we evaluate a long-haul transmission system with strong-mode coupling through simulations, and a short-reach transmission system with weak mode coupling through experiments.

III. SIMULATION RESULTS FOR LONG-HAUL TRANSMISSION

Firstly, we analytically evaluate the performance of DSP-based MDL/MDG estimation in long-haul SDM transmission. Using the multisection model presented in [8], 12×12 matrices \mathbf{H} are generated to simulate a strongly coupled pol-mux 6-mode transmission of 100 50-km spans, yielding a total length of 5,000 km. The group delay standard deviation is set to $3.1 \text{ ps}/\sqrt{\text{km}}$, which is a low value for coupled core MCFs [5], [20]. The MDL/MDG of the link is controlled by a per-amplifier MDG standard deviation, σ_g . Matrices \mathbf{H} are represented by 1,000 frequency bins over a bandwidth of 240 GHz to capture the effect of frequency diversity [21]. The MDG standard deviation σ_{mdg} is estimated in dB using $\mathbf{W}_{\text{MMSE}}^{-1}$ computed from \mathbf{H} using (1). The total MDL/MDG is calculated by averaging over the 1,000 frequency bins. Figs. 2a and 2b show the contour plots of the estimation error in dB for a wide range of SNRs and MDG standard deviations σ_{mdg} , without and with correction of the DSP-estimated eigenvalues, respectively. The estimation error is computed as the absolute difference between the actual and estimated σ_{mdg} in dB. In Fig. 2a, without correction of the DSP-estimated eigenvalues,

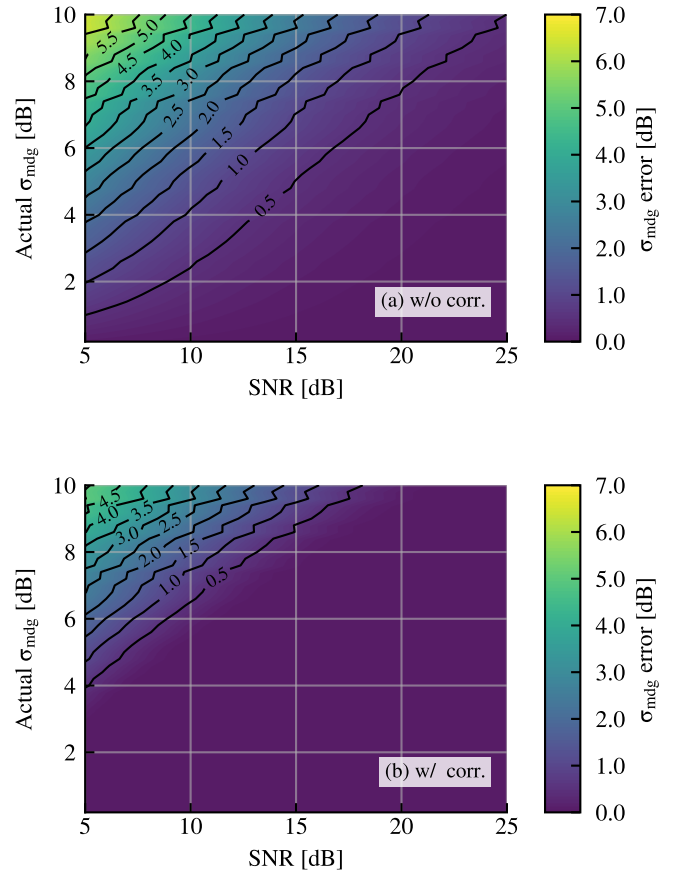


Fig. 2. Analytical estimation error in dB computed as the absolute value of the difference between the actual MDL/MDG standard deviation σ_{mdg} , and the σ_{mdg} estimated in dB using $\mathbf{W}_{\text{MMSE}}^{-1}$ computed from \mathbf{H} using (1). (a) Without correction. (b) Correction by the positive solution of (4).

the estimation error achieves up to 6 dB for $\sigma_{\text{mdg}} > 9$ dB across the low SNR region. At an SNR = 10 dB, an error higher than 1 dB is observed for $\sigma_{\text{mdg}} > 4$ dB. Even at a higher SNR = 15 dB, the estimation error exceeds 1.5 dB for $\sigma_{\text{mdg}} > 8$ dB. The contour plot in Fig. 2a makes evident the SNR impact on the estimation accuracy. In Fig. 2b, the correction of the DSP-estimated eigenvalues by the positive solution of (4) enhances the estimation process. Here, in the low SNR regime, the maximum error is 4.5 dB for $\sigma_{\text{mdg}} > 9$ dB. At an SNR = 10 dB, an error higher than 1 dB is achieved only for $\sigma_{\text{mdg}} > 7$ dB. For $\text{SNR} \geq 19$ dB, the correction factor provides an estimation error below 0.5 dB over the entire range of evaluated σ_{mdg} .

We further simulate a coupled long-haul transmission link with $N_m = 6$ spatial modes and polarization multiplexing, as depicted in the simulation setup of Fig. 3. At the transmitter, $2N_m$ independent binary sequences are mapped into 400,000 16-QAM symbols at 30 Gbd. The complex constellations are fed into root-raised-cosine (RRC) shaped filters with 0.01 roll-off factor, generating an output signal at 8 samples/symbol. The shaped signals are then sent to I/Q Mach-Zehnder modulator (MZM) models for electro-optical conversion. The $2N_m$ optical signals are then launched into the transmission fiber model with strong mode coupling. The

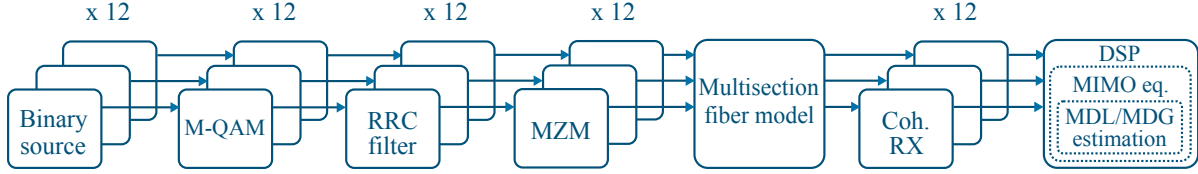


Fig. 3. Simulation setup of coupled long-haul 6-mode transmission. The transmitter generates 16-QAM symbols at 30 GBd. The multisecion model simulates a 5,000-km fiber link. MDL/MDG estimation is performed by DSP based on the MIMO MMSE transfer function.

fiber is modeled using the multisecion scheme presented in [8] for 100 spans and 5,000 km total length. The channel consists of 1,000 frequency bins spread over 240 GHz (note that the simulation bandwidth is 30 GHz times 8 samples per symbol, yielding 240 GHz). The resolution of the channel in frequency domain is adjusted by replicating channel matrices between simulated frequency bins. The group delay standard deviation is set to $3.1 \text{ ps}/\sqrt{\text{km}}$ [20]. The MDL/MDG of the link is controlled by a per-amplifier MDG standard deviation, σ_g . After propagation, the received signals are converted from the optical to the electrical domain by the receiver front-end model. No phase noise has been considered for the simulations. The electric signals are down-sampled to two samples per symbol and fed into the MIMO equalizer for source separation and equalization. 12×12 MIMO equalization is carried out by 144 finite impulse response filters with 100 taps each, updated by a fully supervised least mean squares (LMS) algorithm. The MDG standard deviation σ_{mdg} is computed at each frequency of the MIMO transfer function and averaged across the signal band. MDL/MDG estimation is performed without and with correction factor over the DSP-estimated eigenvalues. Fig. 4a shows σ_{mdg} estimated by the coefficients of the MMSE equalizer as a function of the actual value without correction. In absence of noise, σ_{mdg} estimated from the equalizer coefficients tracks the actual σ_{mdg} with negligible error. As the SNR decreases, the estimation error increases for higher values of σ_{mdg} , underestimating the actual MDL/MDG. Fig. 4b shows that DSP-based MDL/MDG estimation can be significantly improved using the positive correction factor derived in (4), resulting in a small residual error in the investigated range of σ_{mdg} , even for the lowest SNR evaluated.

IV. EXPERIMENTAL SETUP FOR THE 3-MODE TRANSMISSION LINK

The experimental setup used for MDL/MDG emulation is depicted in Fig. 5. At the transmitter, a pseudorandom bit sequence (PRBS) of 2^{16} polarization-multiplexed 16-QAM symbols is generated at 25 GBd. Pulse shaping at the transmitter is done using a RRC filter with 0.01 roll-off factor. The pulse-shaped signal is converted to the analog domain by a 100 GSa/s digital-to-analog converter (DAC) followed by RF-amplifiers. The analog signal modulates the output of an external cavity laser (ECL) operating at a frequency of 193.4 THz with a linewidth of 80 kHz using a dual-polarization in-phase and quadrature modulator. After optical modulation, the signal is amplified by an erbium-doped fiber amplifier (EDFA), split and delayed by 0 m, 20 m and 30 m

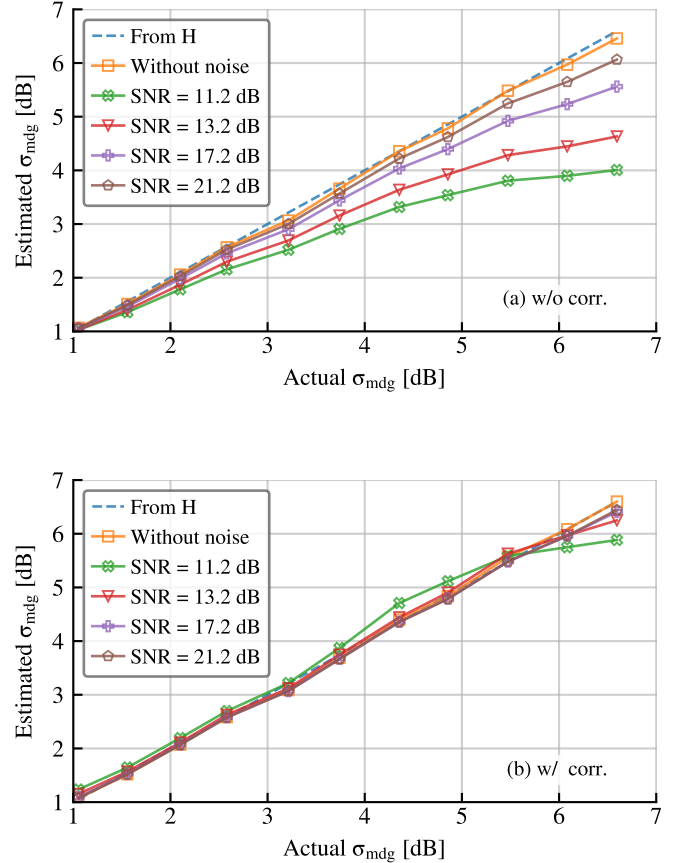


Fig. 4. MDG standard deviation σ_{mdg} estimated from the equalizer coefficients, $\mathbf{W}_{\text{MMSE}}^{-1}$, versus actual σ_{mdg} , at different SNRs. (a) Without correction. (b) Correction by the positive solution of (4).

to generate three decorrelated data streams that are passed through VOAs and then multiplexed by a mode-selective photonic lantern (PL) [23]. The VOAs allow the independent control of the launch powers in the 3 spatial modes LP_{01} , LP_{11a} and LP_{11b} to deliberately introduce MDL/MDG into the system. The output of the PL is an FMF that supports 4 linearly polarized (LP) mode groups. At the receiver side, a second PL is used as mode de-multiplexer. Splicing the FMF pigtailed of the two photonic lanterns results in a 32.5 m link. We also evaluate a longer link by fusion splicing the FMF pigtailed to a 73 km fiber link consisting of 16 spools of 50 μm core diameter graded-index MMF [22] with lengths varying from 1.2 km to 8.9 km. The receiver employs a time domain multiplexed (TDM)-SDM receiver [24] that delays two flows by 3 km and 6 km of standard single-mode fiber (SSMF)

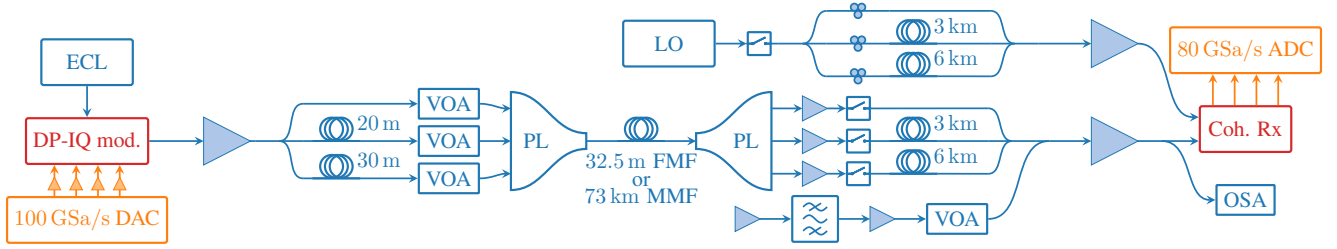


Fig. 5. Experimental setup for MDL/MDG emulation in short-reach 3-mode transmission with polarization multiplexing. The transmitter generates 16-QAM symbols at 25 GBd, which are subsequently split and delayed to create the input tributaries for the PL. VOAs are placed between the delay fibers and the PL inputs in order to emulate MDL/MDG. The multi-mode signal is transmitted over either 32.5 m of 4-LP FMF or over 73 km of MMF [22]. At the receiver, a TDM-SDM scheme is employed, and a noise loading stage is used to vary the OSNR. MDL/MDG estimation is performed in DSP based on the MIMO MMSE transfer function.

TABLE I
VOA ATTENUATION SETTINGS FOR DIFFERENT MDL/MDG EMULATION

Case	Attenuation sweep		
	LP ₀₁	LP _{11a}	LP _{11b}
1	Decreases	Constant at 5 dB	5 dB to 17 dB
2	5 dB to 17 dB	Constant at 5 dB	Decreases
3	Decreases	5 dB to 17 dB	6 dB to 18 dB
4	Decreases	5 dB to 17 dB	5 dB to 17 dB

to reduce the required amount of the coherent receivers. After the TDM-SDM stage, a noise loading stage composed of two EDFAs, a wavelength selective switch (WSS) and a VOA is placed to vary the OSNR at the coherent receiver input. This noise-loading setup places a 250 GHz wide noise-band around the 193.4 THz carrier. The average OSNR is measured by an optical spectrum analyzer (OSA) after the last amplification stage. The SNR at the receiver input is computed as $\text{SNR} = \text{OSNR} (T_s \times 12.5 \text{ GHz})$ where $T_s = 40 \text{ ps}$ is the symbol time [25]. The noisy signal is amplified and converted from the optical to the electrical domain by the receiver frontend that integrates a second ECL as local oscillator (LO). The TDM electric signals are fed into 80 GSa/s analog-to-digital converters (ADC) to be digitized. In the DSP block, the TDM streams are parallelized and down-sampled to two samples per symbol. Next, in case of 73 km transmission, dispersion is digitally compensated and frequency offset is estimated and compensated for. The signal is matched-filtered by a RRC filter, and, finally, decision-directed (DD) equalization is applied. 6×6 MIMO equalization is carried out using a widely linear complex-valued adaptive equalizer, updated by a fully supervised DD-LMS algorithm [26].

V. EXPERIMENTAL RESULTS FOR THE 3-MODE TRANSMISSION LINK

A. MDL/MDG estimation without noise loading

The three VOAs employed to vary the input power for the LP₀₁, LP_{11a}, and LP_{11b} ports of the PL provide an attenuation range from 0 dB to 25 dB for an applied voltage between 0 V and 5 V. Since the relation between the applied voltage and the resulting attenuation is not linear, each individual VOA is calibrated by scanning the applied voltage and measuring the

attenuation. This data is used to generate a lookup table (LUT), which is interpolated to achieve an arbitrary attenuation. At first, the capability of the VOAs to emulate the presence of MDL/MDG in the experimental setup is evaluated. At 0 dB attenuation, for 32.5 m transmission, the launch powers are 0.55 dBm, -0.15 dBm and -0.15 dBm for LP₀₁, LP_{11a} and LP_{11b} ports of the PL, respectively. For transmission over 73 km, the launch powers are measured to be 12.5 dBm, 12.1 dBm and 12.4 dBm for LP₀₁, LP_{11a} and LP_{11b}, respectively. In order to keep the total launch power constant at -4.9 dBm for 32.5 m transmission and 7.3 dBm for 73 km transmission, the 3 VOAs are initialized in 5 dB attenuation to attenuate or de-attenuate the signals according to the configurations defined in Table I. In case 1, the LP_{11b} mode is gradually attenuated, while the attenuation of the LP₀₁ mode decreases in such a way that the total launch power is constant. For case 2, the LP₀₁ mode is attenuated instead of the LP_{11b} mode. In cases 3 and 4, the LP_{11a} and LP_{11b} modes are simultaneously attenuated, while the attenuation over the LP₀₁ mode decreases. The induced MDL/MDG is estimated after DSP from the MIMO transfer function and averaged over 5 different captures. Fig. 6 shows σ_{mdg} as a function of the ratio between the maximum and minimum attenuation for the four cases of Table I. The different attenuation scenarios are used to emulate the system MDL/MDG. From Fig. 6a, at an attenuation ratio of 0 dB, the system has an inherent $\sigma_{\text{mdg}} = 1.3 \text{ dB}$ for 32.5 m transmission, coming from the different launch powers, imperfections of the optical splitters and different insertion losses of the VOAs. In Fig. 6b, for 73 km transmission, a higher inherent $\sigma_{\text{mdg}} = 2.6 \text{ dB}$ is measured as a consequence of the splices connecting the 16 spools. In general, for both 32.5 m and 73 km transmission, the higher the ratio between attenuations, the higher the induced MDL/MDG. In case 2, at low attenuation ratios, the induced MDL/MDG decreases slightly before turning into an increasing curve. Such behavior comes from the fact that, in this configuration, the strongest mode, LP₀₁, is more attenuated than modes LP_{11a} and LP_{11b}, compensating for the inherent launch power differences at 0 dB attenuation. Using cases 3 and 4, σ_{mdg} achieves up to 6 dB as a consequence of the simultaneous attenuation of both LP_{11a} and LP_{11b} modes.

Using the VOAs to experimentally emulate MDL/MDG, Figs. 7a and 7b show the σ_{mdg} estimated by DSP as a function

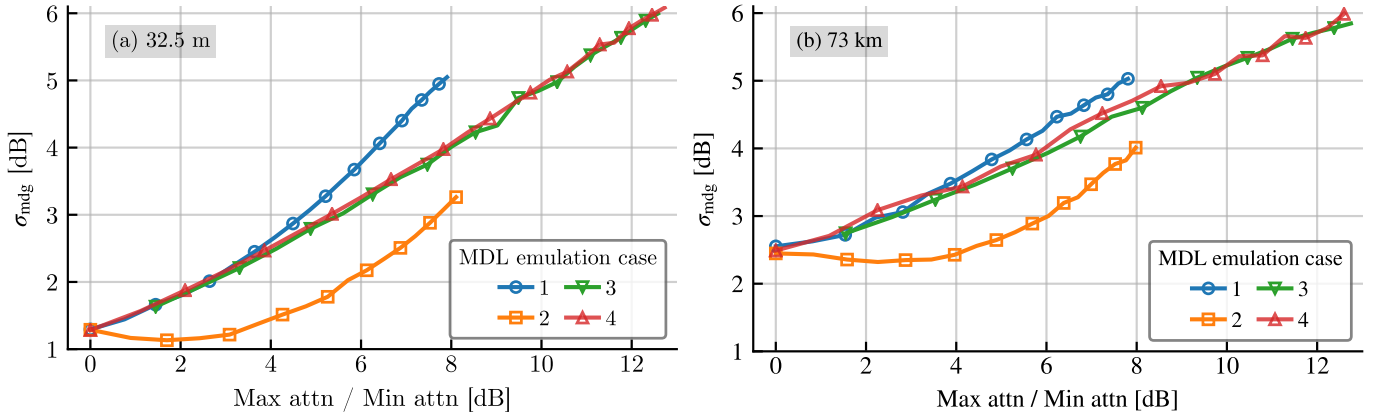


Fig. 6. MDL/MDG standard deviation σ_{mdg} versus attenuation ratio at different MDL/MDG emulation cases, estimated by DSP. (a) Transmission over 32.5 m without noise loading. (b) Transmission over 73 km without noise loading.

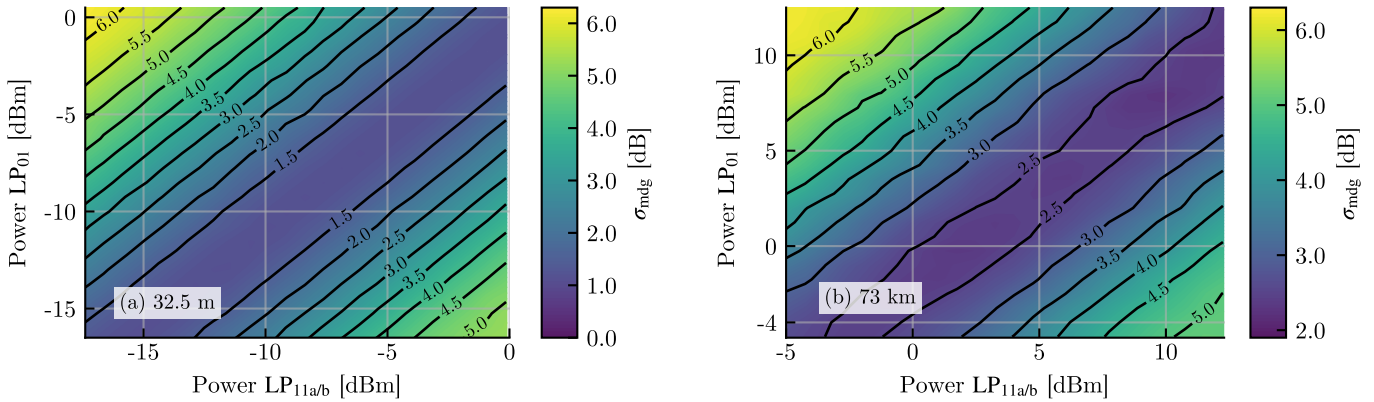


Fig. 7. MDL/MDG standard deviation σ_{mdg} estimated by DSP without noise loading, as a function of the launch powers in the LP₀₁ and LP₁₁ modes. (a) 32.5 m transmission with an intrinsic SNR = 38.5 dB. (b) 73 km transmission with an intrinsic SNR = 37.1 dB.

of the launch powers in the LP₀₁ and LP₁₁ modes achieved by sweeping the attenuation from 0 dB to 17 dB in the 3 VOAs for 32.5 m and 73 km transmission, respectively. In the absence of noise loading, the SNR obtained from the OSNR measured optically by the OSA is 38.5 dB for transmission over 32.5 m and 37.1 dB for transmission over 73 km. From the contour plot in Fig. 7a, σ_{mdg} increases from the middle of the grid towards the top left corner and the bottom right corner, where the difference between the launch powers is maximized. On the contrary, the region encompassing the diagonal between the bottom left corner and the top right corner presents low σ_{mdg} as a consequence of the high similarity between the launch powers. In Fig. 7b, for 73 km transmission, σ_{mdg} also increases in the direction in which the difference between the launch powers is maximized, achieving up to 6.3 dB. Over the region where the launch powers are similar, σ_{mdg} remains low around 2 dB.

B. MDL/MDG estimation with noise loading

We analyze the influence of noise on MDL/MDG estimation by loading noise to the optical transmission setup and calculating the estimation error $\sigma_{\text{mdg}}^{\text{err}}$, defined as the difference

in dB between σ_{mdg} , estimated in the setup without noise loading, and $\sigma_{\text{mdg}}^{\text{nl}}$, estimated with noise loading ($\sigma_{\text{mdg}}^{\text{err}} = \sigma_{\text{mdg}} - \sigma_{\text{mdg}}^{\text{nl}}$).

Figs. 8a and 8b show $\sigma_{\text{mdg}}^{\text{err}}$ for the 32.5 m transmission link, at SNR = 17 dB and SNR = 12 dB. As expected from the simulation results, $\sigma_{\text{mdg}}^{\text{err}}$ for SNR = 17 dB (up to 0.6 dB) is significantly lower than for SNR = 12 dB (up to 1.8 dB). The estimation error after correction is shown in Figs. 8c and 8d for SNR = 17 dB and SNR = 12 dB. The correction factor given by the positive solution of (4) significantly enhances the estimation process over most of the grid, remaining only a small residual error in the high MDL/MDG regime for both SNRs.

The effect of noise on $\sigma_{\text{mdg}}^{\text{err}}$ for 73 km transmission is presented in Figs. 9a and 9b. The estimation error at SNR = 17 dB achieves up to 0.7 dB, while the estimation error at SNR = 12 dB reaches up to 2.2 dB. The estimation error after correction is shown in Figs. 9c and 9d for SNR = 17 dB and SNR = 12 dB, respectively. As observed in the 32.5 m link, the correction factor significantly reduces the estimation error, remaining only a small residual error in the high MDL/MDG regime for both SNRs.

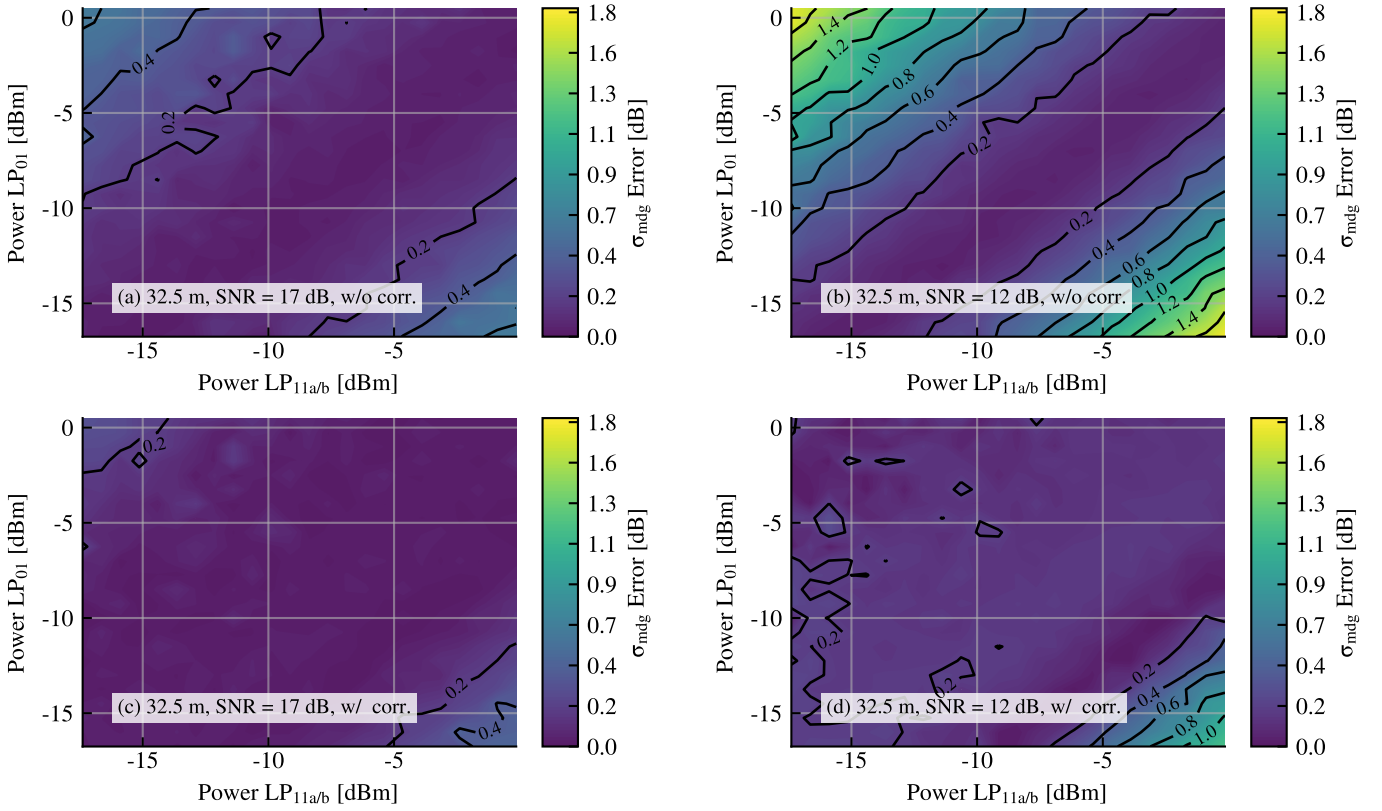


Fig. 8. Estimation error $\sigma_{\text{mdg}}^{\text{err}} = \sigma_{\text{mdg}} - \sigma_{\text{mdg}}^{\text{nl}}$, calculated as the difference in dB between the MDL/MDG standard deviation σ_{mdg} estimated by DSP without noise loading, and $\sigma_{\text{mdg}}^{\text{nl}}$ estimated by DSP with noise loading. In the figure, $\sigma_{\text{mdg}}^{\text{err}}$ is shown as a function of the power launched in the LP₀₁ and LP₁₁ modes for 32.5 m transmission. (a) Without correction at SNR = 17 dB. (b) Without correction at SNR = 12 dB. (c) Correction by the positive solution of (4) at SNR = 17 dB. (d) Correction by the positive solution of (4) at SNR = 12 dB.

Next, we sweep both the attenuation of the VOAs and the noise power at the receiver input. Figs. 10a and 10b show $\sigma_{\text{mdg}}^{\text{err}}$ as a function of σ_{mdg} and SNR without and with correction of the DSP-estimated eigenvalues for 32.5 m transmission. In Fig. 10a, without correction, the estimation error achieves up to 1.8 dB for $\sigma_{\text{mdg}} > 6$ dB and SNR < 12 dB. At an SNR = 12 dB, the estimation error varies from 0.25 dB to 1.7 dB across the range $2 \text{ dB} < \sigma_{\text{mdg}} < 6$ dB. As the SNR increases, the estimation error decreases progressively. At an SNR > 20.5 dB, the estimation error is less than 0.25 dB for all ranges of σ_{mdg} . The correction factor applied over the DSP-estimated eigenvalues enhances the estimation across all ranges of σ_{mdg} and SNR evaluated in Fig. 10b. Here, a residual error of 0.2 dB is achieved for the high MDL/MDG regime. For SNR < 12 dB, the residual error is negative as a consequence of the over-correction of the eigenvalues that results in an estimated σ_{mdg} higher than the actual σ_{mdg} . The results for 73 km transmission are shown in Figs. 10c and 10d. In Fig. 10c, without correction, the estimation error achieves up to 2 dB for $\sigma_{\text{mdg}} > 6$ dB and SNR < 12 dB. At an SNR = 12 dB, the estimation error varies from 0.75 dB to 1.75 dB across the range $3.5 \text{ dB} < \sigma_{\text{mdg}} < 6$ dB. An estimation error less than 0.25 dB for all values of σ_{mdg} is obtained for SNR values higher than 22 dB. The correction factor significantly reduces the estimation error, as shown in Fig. 10d. In this case, only a residual error of 0.2 dB is observed in certain regions

of the grid. For SNR < 12 dB and $3.7 \text{ dB} < \sigma_{\text{mdg}} < 5.2$ dB, there is a negative residual error of -0.2 dB as a consequence of over-correction.

VI. CONCLUSION

In space division multiplexing (SDM) systems with coupled channels, the achievable channel capacity and transmission distance are fundamentally constrained by noise, mode-dependent loss (MDL) and mode-dependent gain (MDG). MDL/MDG not only reduce the average capacity but can cause outages. MDL/MDG estimation carried out by coherent receivers is a useful tool for link assessment and troubleshooting. In this paper, we show that MDL/MDG estimation carried out directly from the dynamic equalizer coefficients is prone to errors in regimes of low signal-to-noise ratio (SNR) and high MDL/MDG. Using the transfer function of an equalizer based on the minimum mean square error (MMSE) criterion, we calculate a correction factor that improves the estimation process in moderate levels of MDG/MDL and SNRs. We validate the correction method by Monte-Carlo simulations of a 6-mode long-haul coupled transmission processed by a 12×12 dynamic equalizer. Moreover, we experimentally validate the correction factor in a 3-mode transmission link using the coefficients of a 6×6 dynamic equalizer for both 32.5 m and 73 km transmission. The simulations and exper-

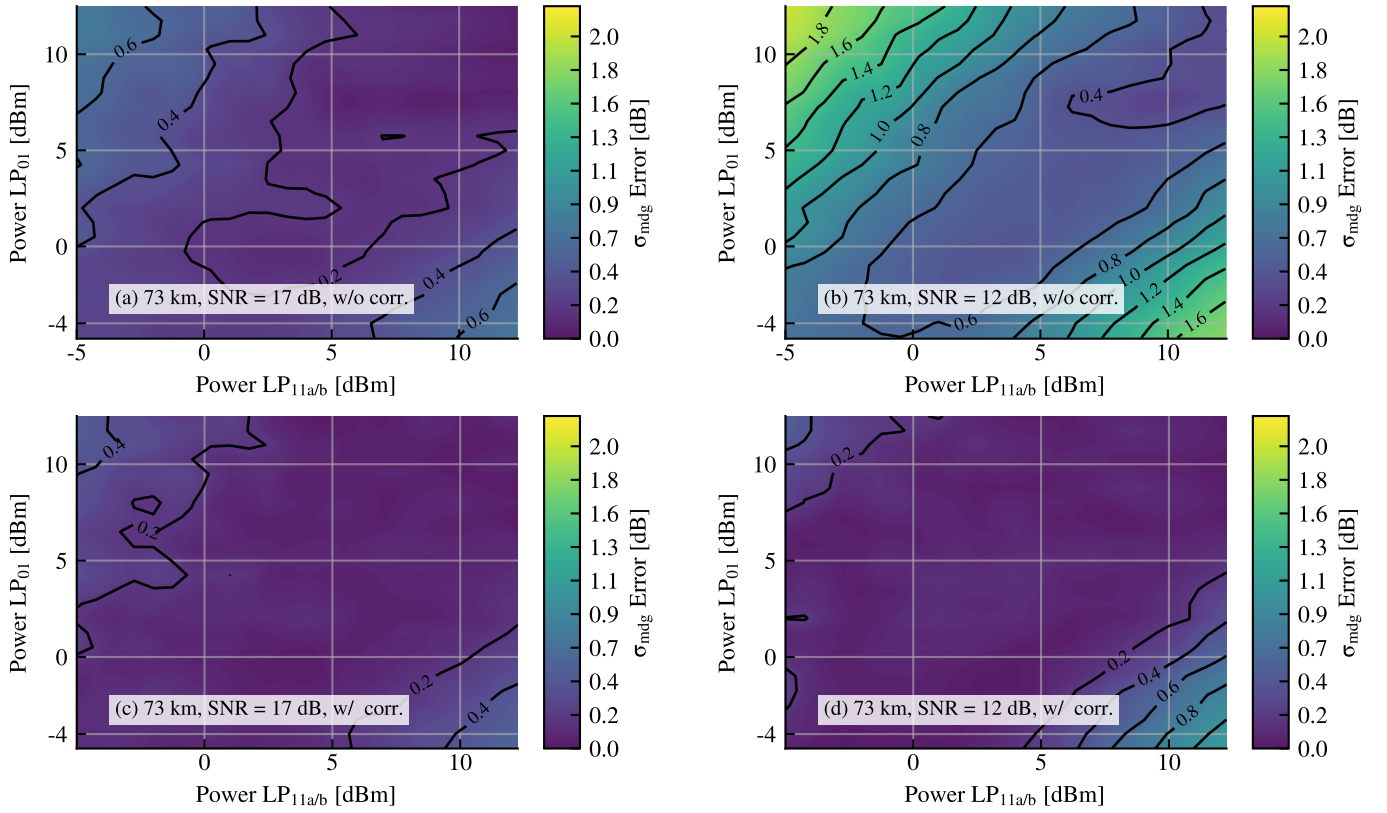


Fig. 9. Estimation error $\sigma_{\text{mdg}}^{\text{err}} = \sigma_{\text{mdg}} - \sigma_{\text{mdg}}^{\text{nl}}$, calculated as the difference in dB between the MDL/MDG standard deviation σ_{mdg} estimated by DSP without noise loading, and $\sigma_{\text{mdg}}^{\text{nl}}$ estimated by DSP with noise loading. In the figure, $\sigma_{\text{mdg}}^{\text{err}}$ is shown as a function of the power launched in the LP₀₁ and LP₁₁ modes for 73 km transmission. (a) Without correction at SNR = 17 dB. (b) Without correction at SNR = 12 dB. (c) Correction by the positive solution of (4) at SNR = 17 dB. (d) Correction by the positive solution of (4) at SNR = 12 dB.

iments confirm the applicability of the method in practical transmission scenarios.

REFERENCES

- [1] P. Winzer and G. Foschini, "Optical MIMO-SDM system capacities," in *Optical Fiber Communication Conference*. IEEE, 2014, pp. Th1J–1.
- [2] A. C. Jatoba-Neto, D. A. A. Mello, C. E. Rothenberg *et al.*, "Scaling SDM optical networks using full-spectrum spatial switching," *IEEE/OSA Journal of Optical Communications and Networking*, vol. 10, no. 12, pp. 991–1004, 2018.
- [3] O. D. Domingues, D. A. A. Mello, R. da Silva *et al.*, "Achievable rates of space-division multiplexed submarine links subject to nonlinearities and power feed constraints," *Journal of Lightwave Technology*, vol. 35, no. 18, pp. 4004–4010, 2017.
- [4] K. Igarashi, D. Souma, Y. Wakayama *et al.*, "114 space-division-multiplexed transmission over 9.8-km weakly-coupled-6-mode uncoupled-19-core fibers," in *Optical Fiber Communication Conference*. Optical Society of America, 2015, pp. Th5C–4.
- [5] R. Ryf, J. C. Alvarado-Zacarias, S. Wittek *et al.*, "Coupled-core transmission over 7-core fiber," in *Optical Fiber Communication Conference*. Optical Society of America, 2019, pp. Th4B–3.
- [6] J. van Weerdenburg, R. Ryf, J. C. Alvarado-Zacarias *et al.*, "138-Tb/s mode-and wavelength-multiplexed transmission over six-mode graded-index fiber," *Journal of Lightwave Technology*, vol. 36, no. 6, pp. 1369–1374, 2018.
- [7] D. Soma, Y. Wakayama, S. Beppu *et al.*, "10.16 peta-bit/s dense SDM/WDM transmission over low-DMD 6-mode 19-core fibre across C+L band," in *2017 European Conference on Optical Communication (ECOC)*. IEEE, 2017, pp. 1–3.
- [8] K.-P. Ho and J. M. Kahn, "Mode-dependent loss and gain: statistics and effect on mode-division multiplexing," *Optics express*, vol. 19, no. 17, pp. 16612–16635, 2011.
- [9] P. J. Winzer and G. J. Foschini, "MIMO capacities and outage probabilities in spatially multiplexed optical transport systems," *Optics express*, vol. 19, no. 17, pp. 16680–16696, 2011.
- [10] D. A. A. Mello, H. Srinivas, K. Choutagunta *et al.*, "Impact of polarization- and mode-dependent gain on the capacity of ultra-long-haul systems," *Journal of Lightwave Technology*, vol. 38, no. 2, pp. 303–318, 2020.
- [11] J. van Weerdenburg, R. Ryf, J. C. Alvarado-Zacarias *et al.*, "138 Tbit/s transmission over 650 km graded-index 6-mode fiber," in *2017 European Conference on Optical Communication (ECOC)*. IEEE, 2017, pp. 1–3.
- [12] G. Rademacher, R. Ryf, N. K. Fontaine *et al.*, "Long-haul transmission over few-mode fibers with space-division multiplexing," *Journal of Lightwave Technology*, vol. 36, no. 6, pp. 1382–1388, 2018.
- [13] G. Rademacher, B. J. Puttnam, R. S. Luís *et al.*, "10.66 Peta-Bit/s transmission over a 38-core-three-mode fiber," in *Optical Fiber Communication Conference*. Optical Society of America, 2020, pp. Th3H–1.
- [14] R. S. Ospina, C. Okonkwo, and D. A. Mello, "DSP-based mode-dependent loss and gain estimation in coupled SDM transmission," in *Optical Fiber Communication Conference*. Optical Society of America, 2020, pp. W2A–47.
- [15] M. S. Faruk and S. J. Savory, "Digital signal processing for coherent transceivers employing multilevel formats," *Journal of Lightwave Technology*, vol. 35, no. 5, pp. 1125–1141, 2017.
- [16] A. Lobato, F. Ferreira, J. Rabe *et al.*, "Mode scramblers and reduced-search maximum-likelihood detection for mode-dependent-loss-impaired transmission," in *2013 European Conference and Exhibition on Optical Communication (ECOC 2013)*. IET, 2013, pp. 1–3.
- [17] K. Choutagunta, S. Ö. Arik, K.-P. Ho *et al.*, "Characterizing mode-dependent loss and gain in multimode components," *Journal of Lightwave Technology*, vol. 36, no. 18, pp. 3815–3823, 2018.
- [18] N. Kim, Y. Lee, and H. Park, "Performance analysis of MIMO system with linear MMSE receiver," *IEEE Transactions on Wireless Communications*, vol. 7, no. 11, pp. 4474–4478, 2008.
- [19] M. R. McKay, I. B. Collings, and A. M. Tulino, "Achievable sum

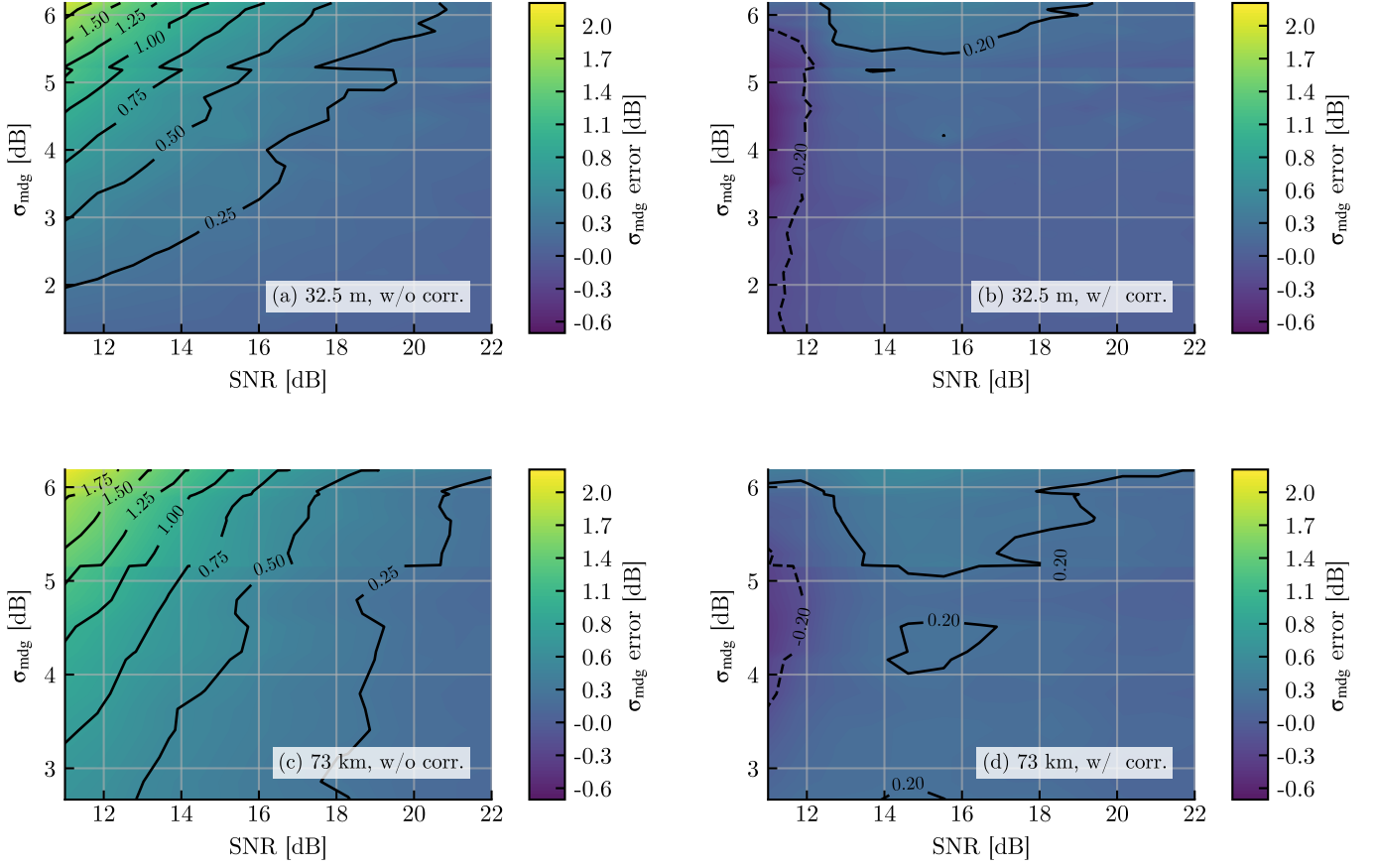


Fig. 10. Estimation error $\sigma_{\text{mdg}}^{\text{err}} = \sigma_{\text{mdg}} - \sigma_{\text{mdg}}^{\text{nl}}$, calculated as the difference in dB between the MDL/MDG standard deviation σ_{mdg} estimated by DSP without noise loading, and $\sigma_{\text{mdg}}^{\text{nl}}$ estimated by DSP with noise loading. In the figure, $\sigma_{\text{mdg}}^{\text{err}}$ is shown as a function of σ_{mdg} and the SNR. (a) 32.5 m transmission without correction. (b) 32.5 km transmission with correction by the positive solution of (4). (c) 73 km transmission without correction. (d) 73 km transmission with correction by the positive solution of (4).

- rate of MIMO MMSE receivers: A general analytic framework,” *IEEE Transactions on Information Theory*, vol. 56, no. 1, pp. 396–410, 2009.
- [20] T. Hayashi, Y. Tamura, T. Hasegawa *et al.*, “Record-low spatial mode dispersion and ultra-low loss coupled multi-core fiber for ultra-long-haul transmission,” *Journal of Lightwave Technology*, vol. 35, no. 3, pp. 450–457, 2017.
- [21] K.-P. Ho and J. M. Kahn, “Frequency diversity in mode-division multiplexing systems,” *Journal of Lightwave Technology*, vol. 29, no. 24, pp. 3719–3726, 2011.
- [22] P. Sillard, D. Molin, M. Bigot-Astruc *et al.*, “50 μm multimode fibers for mode division multiplexing,” *Journal of Lightwave Technology*, vol. 34, no. 8, pp. 1672–1677, 2016.
- [23] A. M. Velázquez Benítez, J. E. Antonio López, J. C. Alvarado Zacarías *et al.*, “Scaling photonic lanterns for space-division multiplexing,” *Scientific reports*, vol. 8, no. 1, pp. 1–9, 2018.
- [24] R. Van Uden, R. A. Correa, E. A. Lopez *et al.*, “Ultra-high-density spatial division multiplexing with a few-mode multicore fibre,” *Nature Photonics*, vol. 8, no. 11, p. 865, 2014.
- [25] R.-J. Essiambre, G. Kramer, P. J. Winzer *et al.*, “Capacity limits of optical fiber networks,” *Journal of Lightwave Technology*, vol. 28, no. 4, pp. 662–701, 2010.
- [26] E. P. da Silva and D. Zibar, “Widely linear equalization for IQ imbalance and skew compensation in optical coherent receivers,” *Journal of Lightwave Technology*, vol. 34, no. 15, pp. 3577–3586, 2016.